High-order computation of incompressible flow on arbitrarily moving unstructured meshes using direct discontinuous Galerkin formulation

E. Lee [*], H. T. Ahn [*], H. Luo [**] and J. Cheng [***]
Corresponding author: htahn@ulsan.ac.kr

* School of Naval Architecture and Ocean Engineering, University of Ulsan, Republic of Korea
** Department of Mechanical and Aerospace Engineering, North Carolina State University, USA
*** School of Mathematics and Systems Science, Beihang University, P.R. China

Abstract: The direct discontinuous Galerkin method is used to calculate the viscous flux and the Arbitrary Lagrangian-Eulerian method is adopted so that the fluid analysis domain changes over time. To calculate the higher order numerical flux, we reconstructed the solution using the solution information. First, the Taylor-Green vortex problem is analyzed to confirm the performance of the fluid solver without Arbitrary Lagrangian Eulerian. Second, the flow past a circular cylinder problem is analyzed to confirm the performance of Arbitrary Lagrangian Eulerian solver.

Keywords: Computational Fluid Dynamics, Direct Discontinuous Galerkin, Fluid-Structure Interaction, Finite Volume Method.

1   Introduction

When an object having a thickness is enclosed by a fluid, a vortex is generated behind the object. The vortex occurs when the stagnation pressure acting on the front of the object is lost due to friction between the object and the fluid. This vortex appearance is highly nonlinear. Such non-forming fluid behavior causes the object to vibrate. Such a vibration phenomenon is referred to as a Vortex-Induced Vibration.

The main mechanism by which the vortex-induced vibration occurs is the friction due to the viscosity of the fluid. Therefore, in order to numerically simulate the vortex-induced vibration, it is necessary to predict the viscosity of the fluid robustly and accurately. In this study, we try to simulate the viscosity of a fluid using Direct Discontinuous Galerkin method. If this method is used, it is expected that the viscosity of the fluid can be predicted with a high order of accuracy in a spatial domain.[1-3]

2   Governing Equations

Non-dimensionalized Navier-Stokes equations for incompressible flows in an arbitrarily moving domain can be written as follows,

$$\frac{d}{dt^*} \int_{\Omega} \boldsymbol{Q} dV + + \frac{d}{dt} \int_{\Omega} \boldsymbol{U} dV + \oint_{\partial\Omega} \boldsymbol{F} \cdot \boldsymbol{n} dS = \oint_{\partial\Omega} \boldsymbol{G} \cdot \boldsymbol{n} dS$$

$$where\ \boldsymbol{Q} = \left\{ \begin{matrix} p/\beta \\ u_i \end{matrix} \right\}, \boldsymbol{U} = \left\{ \begin{matrix} 1 \\ u_i \end{matrix} \right\}, \boldsymbol{F}_j = \left\{ \begin{matrix} u_j - v_j \\ u_i(u_j - v_j) + p\delta_{ij} \end{matrix} \right\}, \boldsymbol{G}_j = \left\{ \begin{matrix} 0 \\ \frac{1}{Re}(u_{i,j} + u_{j,i}) \end{matrix} \right\}$$

Where the unknowns are the velocity vector $\boldsymbol{u}$, the pressure p, and the velocity vector of moving domain $\boldsymbol{v}$. The above equations are rewritten by introducing the artificial compressibility term in pseudo time t^*.

3   Finite Volume Formulation

Governing equations are discretized using Finite Volume Formulation as follows:

$$\frac{d}{dt^*}(\bar{Q}_i\Omega_i) + \frac{d}{dt}(\bar{U}_i\Omega_i) + \sum_{j=1}^{N_{nei}} F_j^{invc}(Q_L, Q_R; n_{ij}) \cdot \Delta s_{ij} = \sum_{j=1}^{N_{nei}} G_j^{visc}(\nabla Q_L, \nabla Q_R; n_{ij}) \cdot \Delta s_{ij}$$

In the above equation $\bar{Q}_i, \bar{U}_i$ are volume averaged quantities such as,

$$\bar{Q}_i = \frac{1}{\Omega_i} \int_{\Omega_i} Q(x, y)dV,$$

$$\bar{V}_i = \frac{1}{\Omega_i} \int_{\Omega_i} V(x, y)dV$$

For a viscous flux, $\boldsymbol{G}_j^{visc}$ is computed by direct discontinuous Galerkin method[2,3] such as,

$$\boldsymbol{G}_j^{visc}(U_L, \nabla U_L, U_R, \nabla U_R; n_j) = G_j^{visc}(\widehat{U}_x, \widehat{U}_x)$$
$$where\ \widehat{U}_x = \beta_0 \frac{[U]}{\Delta} n_x + \overline{\partial_x U} + \beta_1 \Delta([\partial_{xx}U]n_x + [\partial_{xy}U]n_y),$$
$$\widehat{U}_y = \beta_0 \frac{[U]}{\Delta} n_y + \overline{\partial_y U} + \beta_1 \Delta([\partial_{yx}U]n_x + [\partial_{yy}U]n_y).$$

In the above equations $\overline{\partial_x U}, \overline{\partial_y U}$ are the average, $[U]$ is the jump of solution U, $[\partial_{xx}U]$, $[\partial_{xy}U]$, $[\partial_{yx}U], [\partial_{yy}U]$ are the jump of the second derivation of solution U, Δ is the characteristic length of an interface, and β_0, β_1 are coefficient.

For inviscid flux $\boldsymbol{F}_j^{invc}$ is computed by Roe's flux difference scheme such as,

$$\boldsymbol{F}_{Roe}(\boldsymbol{Q}_L^k, \boldsymbol{Q}_R^k; \widehat{\boldsymbol{n}}) = \frac{1}{2}\left(\boldsymbol{F}(\boldsymbol{Q}_L^k; \widehat{\boldsymbol{n}}) + \boldsymbol{F}(\boldsymbol{Q}_R^k; \widehat{\boldsymbol{n}})\right) + \frac{1}{2}|\widehat{\boldsymbol{A}}(\boldsymbol{Q}_L^k, \boldsymbol{Q}_R^k; \widehat{\boldsymbol{n}})|(\boldsymbol{Q}_R^k - \boldsymbol{Q}_L^k).$$

4   Implicit Time Discretization

The pseudo-time is discretized using 1st order Backward Differentiation Formula. And real-time is discretized using the 2nd order Backward Differentiation Formula.

$$V_i \frac{\Delta \boldsymbol{Q}_i^n}{\Delta t^*} + V_i \frac{3V_i^{n+1} - 4V_i^n + V_i^{n-1}}{2\Delta t} = -\boldsymbol{R}_i^{*n+1},$$

$$where\ -\boldsymbol{R}_i^{*n+1} = \sum_{j=1}^{N_{nei}} G_j^{visc}(\nabla Q_L, \nabla Q_R; n_{ij}) \cdot \Delta s_{ij} - \sum_{j=1}^{N_{nei}} F_j^{invc}(Q_L, Q_R; n_{ij}) \cdot \Delta s_{ij}$$

Right-hand side term of above equation $\boldsymbol{R}$ is residual of a solution. Residual is can be expressed in 1st order formula like,

$$R^{*n+1}_i = \left(R^{*n}_i + \frac{\partial R^{*n}_i}{\partial Q} \Delta Q^n_i \right).$$

Due to the above relation, the unknowns of the equation changed from solutions to solution increment like,

$$\left(\frac{I}{\Delta t^*} V_i + \frac{\partial R^{*n}_i}{\partial Q} \right) \Delta Q^n_i = -R^{*n}_i - V_i \frac{3V^{n+1}_i - 4V^n_i + V^{n-1}_i}{2\Delta t}.$$

5   Results

5.1   Taylor Green vortex

The Taylor-Green vortex analysis was performed to verify the unsteady solver. The analytical solution of Taylor-Green vortex is as follows.

$$u = \sin(x)\cos(y)\, e^{-\frac{2t}{Re}},$$
$$v = -\cos(x)\sin(y)\, e^{-\frac{2t}{Re}},$$
$$p = \frac{1}{4}\cos(2x)\cos(2y)\, e^{-\frac{4t}{Re}}$$

5.2.1   Structured mesh

First, the analysis was performed on the structured mesh which has good uniformity, that is, Cartesian mesh. In the case of such a grid, the maximum performance of the algorithm can be confirmed. The Reynolds number in this analysis is set at 1000,000.
The analysis was performed on a more fine mesh to check the order of accuracy. The results are shown in Figure 2 and Table 1. The result was measured when the real time was 1.
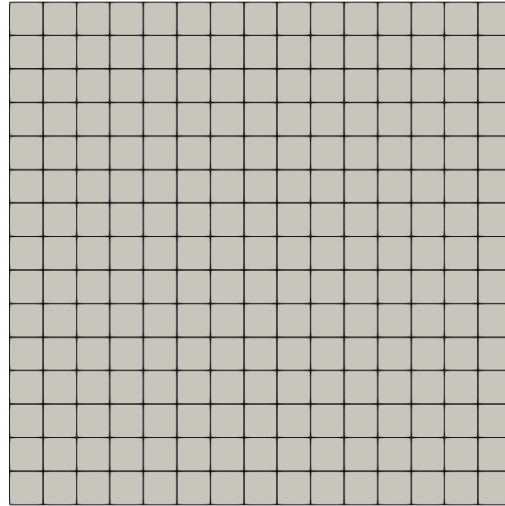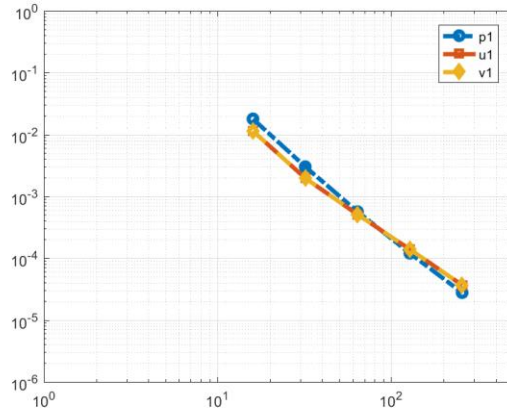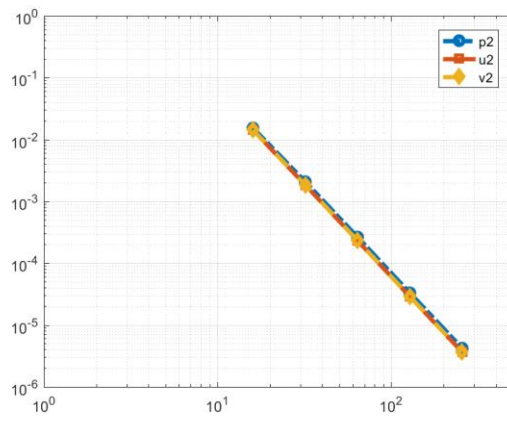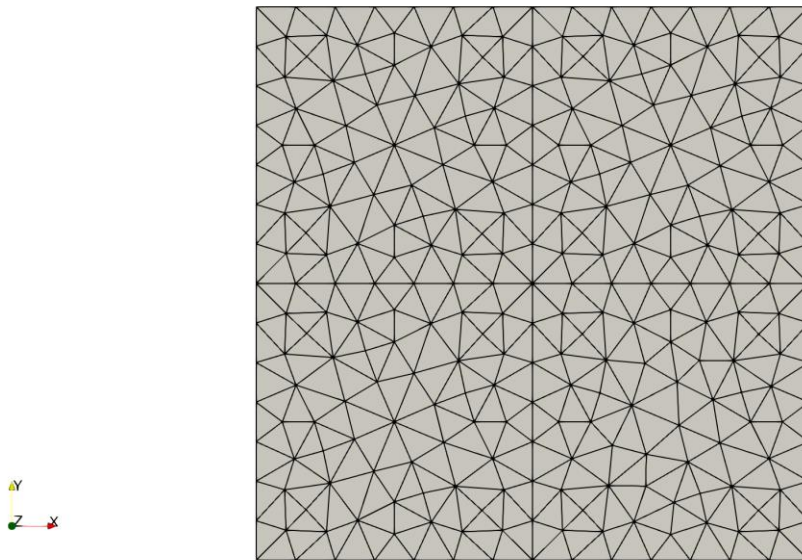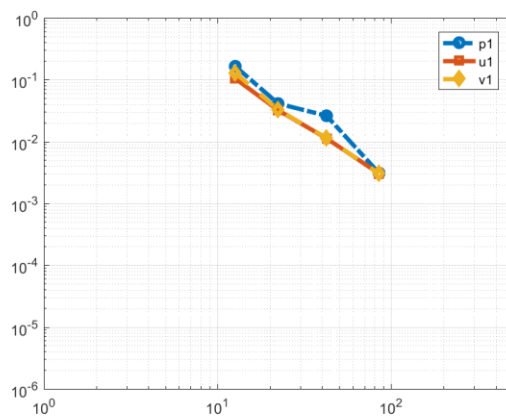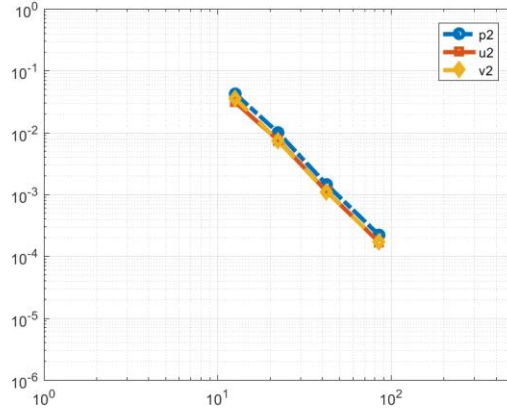

Figure 1. Structured mesh

(a) 1st order reconstruction

(b) 2nd order reconstruction

Figure 2. Results of mesh refinement and order of convergence study using the structured mesh

Table 1. Errors and order of accuracy at each step of mesh refinement using structured mesh.

	ncells	p		u		v	
		L2 Error	order of accuracy	L2 Error	order of accuracy	L2 Error	order of accuracy
P1	256	1.79E-02	-	1.14E-02	-	1.14E-02	-
	1024	3.02E-03	2.57	1.97E-03	2.53	1.97E-03	2.53
	4096	5.66E-04	2.42	5.10E-04	1.95	5.10E-04	1.95
	16384	1.20E-04	2.24	1.39E-04	1.88	1.39E-04	1.88
	65536	2.77E-05	2.12	3.67E-05	1.92	3.67E-05	1.92
P2	256	1.54E-02	-	1.43E-02	-	1.43E-02	-
	1024	2.08E-03	2.89	1.85E-03	2.95	1.85E-03	2.95
	4096	2.64E-04	2.98	2.31E-04	3.00	2.31E-04	3.00
	16384	3.31E-05	3.00	2.89E-05	3.00	2.89E-05	3.00
	65536	4.22E-06	2.97	3.66E-06	2.98	3.66E-06	2.98

From the analysis results, it can be seen that the order of accuracy at p1 is almost 2 and that at p2 is 3.

5.2.1 Unstructured mesh

Second, the analysis was performed on the unstructured mesh. The Reynolds number in this analysis is set at 1000,000.
The analysis was performed on a more fine mesh to check the order of accuracy. The results are shown in Figure 4 and Table 2. The result was measured when the real time was 1.

Figure 3. Unstructured mesh

(a) P1

(b) P2

Figure 4. Results of mesh refinement and order of convergence study using unstructured mesh

Table 2. Errors and order of accuracy at each step of mesh refinement using unstructured mesh.

	ncells	p		u		v	
		L2 Error	order of accuracy	L2 Error	order of accuracy	L2 Error	order of accuracy
P1	160	1.65E-01	-	1.05E-01	-	1.29E-01	-
	498	4.12E-02	2.45	3.22E-02	2.08	3.28E-02	2.41
	1802	2.61E-02	0.71	1.13E-02	1.63	1.14E-02	1.64
	7246	3.08E-03	3.07	3.03E-03	1.89	3.04E-03	1.90
P2	160	4.23E-02	-	3.10E-02	-	3.56E-02	-
	498	1.00E-02	2.54	7.54E-03	2.49	7.34E-03	2.78
	1802	1.44E-03	3.01	1.12E-03	2.97	1.10E-03	2.95
	7246	2.20E-04	2.71	1.68E-04	2.72	1.70E-04	2.69

Vorticity value was calculated from the analysis results. Vorticity is defined as follows:

$$\omega = \frac{\partial v}{\partial x} - \frac{\partial u}{\partial y}$$
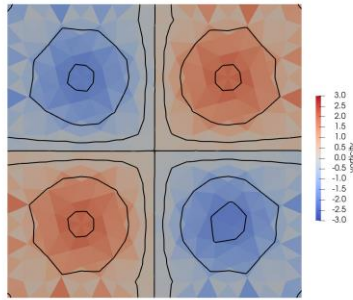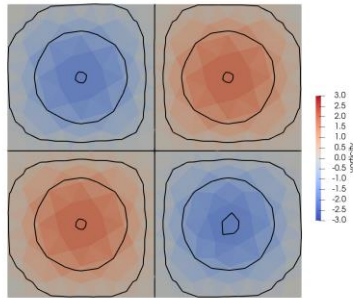
The vorticity contour is shown in figure 5.
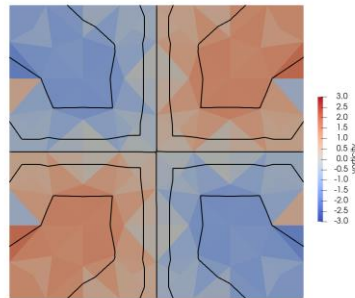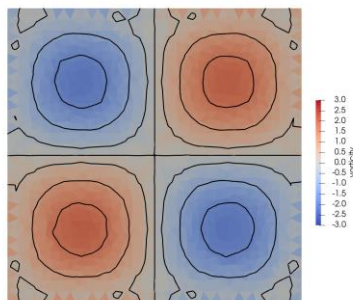

(a) mesh level 1 – P1
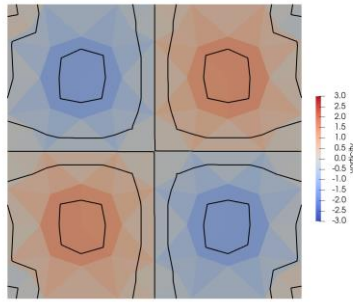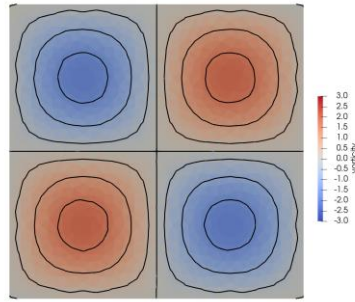
(b) mesh level 1 – P2
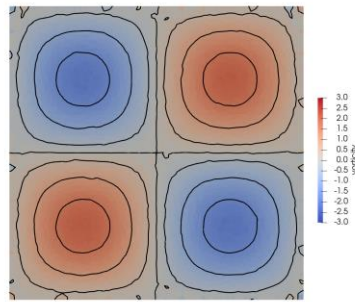

(c) mesh level 2 – P1

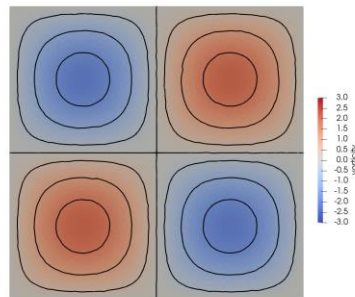

(d) mesh level 2 – P2

(e) mesh level 3 – P1

(f) mesh level 3 – P2

(e) mesh level 4 – P1

(f) mesh level 4 – P2
Figure 5. Vorticity contour

From the analysis results, it can be seen that the order of accuracy at p1 is less than that of the structured mesh. Especially, at level 3, the order of accuracy is small, which seems to be due to the uniformity of the mesh.

The vorticity contour shows the effect of high-order flux reconstruction. Analysis results show that 2nd order reconstruction at the same mesh level can better capture the vortex.

5.2   Flow past a circular cylinder

The flow past a circular cylinder analysis was performed to verify the arbitrary Lagrangian-Eulerian solver.

5.2.1   Fixed circular cylinder

First, the flow past a fixed circular cylinder analysis was performed. Figure 6 shows how the Strouhal number varies with Reynolds number.
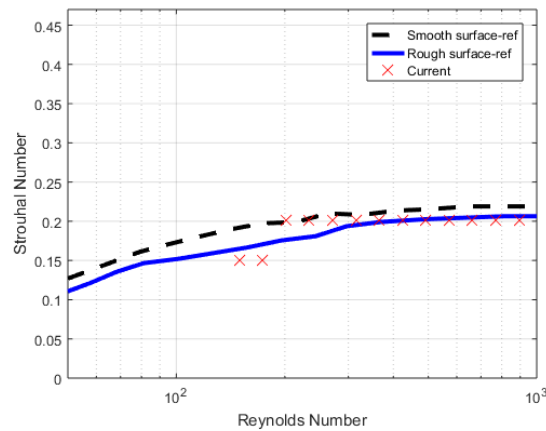

Figure 6. Change of the Strouhal number according to the Reynolds number(Fixed cylinder)

The analysis results show that the Strouhal number is similar to that of other researchers.

5.2.2   Moving circular cylinder (1 degrees of freedom)

Second, the flow past a moving circular cylinder analysis was performed. The motion of the cylinder is assumed to be one degree of freedom as the following equation.

$$\ddot{y} + \left(\frac{4\pi^2}{U_{red}^2}\right)y = \left(\frac{1}{2M_{red}}\right)C_L(t)$$

Where $U_{red} = \frac{U_\infty}{f_n}$, $M_{red} = \frac{m}{\rho_\infty D^2}$

$$M\ddot{y} + Ky = R$$

The fluid analysis solver and the cylinder motion analysis solver are coupled as shown in the following algorithm. Figure 9 shows how the Strouhal number varies with Reynolds number. From the analysis results, it can be seen that the Strouhal number is smaller than that of 5.2.1 which fixed the cylinder. This seems to be because the force acting on the cylinder by the fluid was used to move the cylinder.
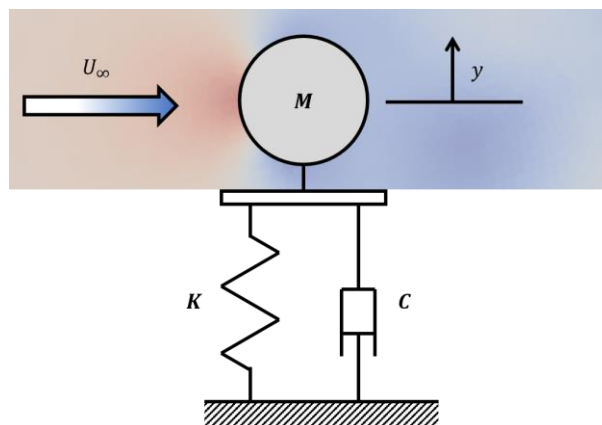
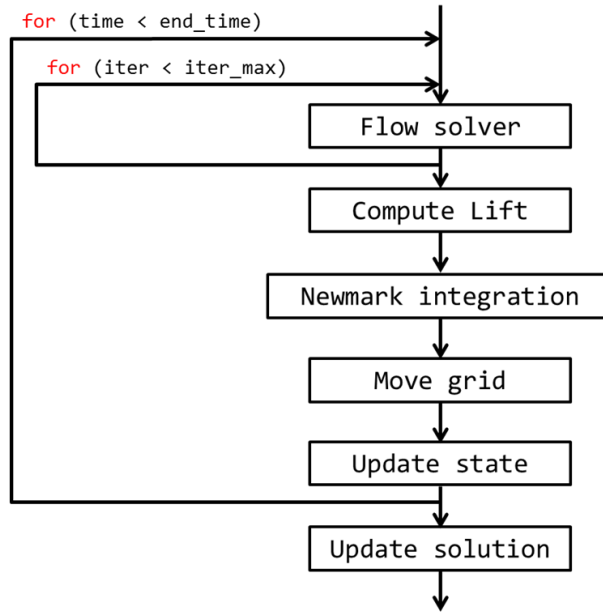

Figure 7. Schematic diagram of numerical analysis
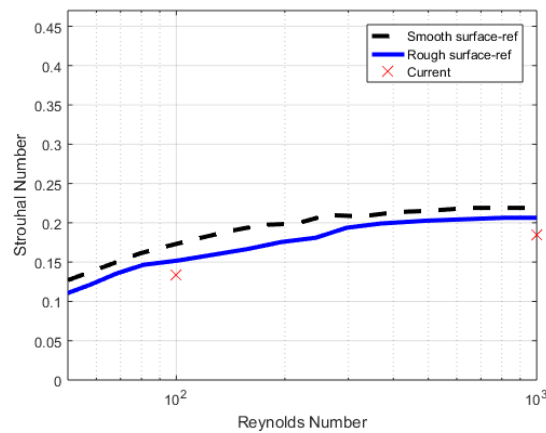
9

Figure 8. Coupling algorithm

Figure 9. Change of the Strouhal number according to the Reynolds number (Moving cylinder)

5 Conclusion and Future Work

The direct discontinuous Galerkin method is used to calculate the viscous flux and the Arbitrary Lagrangian-Eulerian method is adopted so that the fluid analysis domain changes over time. To calculate the higher order numerical flux, we reconstructed the solution using the solution information.

First, the Taylor-Green vortex problem is analyzed to confirm the performance of the fluid solver without Arbitrary Lagrangian Eulerian. From the results of the analysis, it can be seen that although the performance is slightly degraded according to the uniformity of the mesh, the order of accuracy is generally good.

Second, the flow past a circular cylinder problem is analyzed to confirm the performance of Arbitrary Lagrangian Eulerian solver. The motion of the cylinder was fixed with one degree of freedom, and the results of the analysis showed that the result was generally reasonable.

However, since the simulation case is rather small, additional simulation is necessary to

make a conclusion.

References

[1] E. Lee and H.T. Ahn. A reconstruction-based cell-centered high-order finite volume method for incompressible viscous flow simulation on unstructured meshes Com. & Fluid, under review, 2018.

[2] H. Liu and J. Yan. The Direct Discontinuous Galerkin (DDG) Methods for Diffusion Problems. SIAM J. on Num. Analysis, 47(1):675-698, 2009.

[3] H. Luo. A reconstructed discontinuous Galerkin method for the compressible Navier-Stokes equations on arbitrary grids. J. Comp. Physics, 229(19):6961-6978, 2010.

[4] H. T. Ahn. Strongly coupled flow/structure interactions with a geometrically conservative ALE scheme on general hybrid meshes. J. Comp. Physics, 219(2):671-696, 2006.